Platform for Incisionless, Focal, and Multisite Brain Interventions

Taylor D. Webb[1], Matthew G. Wilson[1], Henrik Odéen[2], and Jan Kubanek[1]

[1]Department of Biomedical Engineering, University of Utah
[2]Department of Radiology and Imaging Sciences, University of Utah

ABSTRACT

Precision healthcare treats disease at its source, maximizing treatment efficacy while minimizing side effects. Transcranial focused ultrasound brings this methodology to the human brain, delivering focal interventions to deep brain sites without the need for surgeries. Depending on stimulus duration, ultrasound modulates neural activity—which is useful for systematic diagnoses of disease sources—or induces plastic changes and so a durable reset of the sources. In addition, ultrasound can be applied to selectively deliver drugs into specific targets, thus increasing treatment efficacy while sparing other tissues and organs from potential side effects. The agents can be delivered either across an intact blood brain barrier (small drugs) or across a blood brain barrier that is transiently opened by ultrasound (large drugs, genes, stem cells). Clinical translation of these groundbreaking approaches requires a practical system that can deliver ultrasound into specific brain targets on command. We developed a platform with these features and validated its function in nonhuman primates. In particular, we used the platform to modulate two deep brain nuclei—the left and the right lateral geniculate nucleus–during visual choice behavior. We found that specific stimulation parameters reliably yet reversibly modulated the choice behavior. This platform is being used to systematically investigate the space of effective stimulation parameters for transient and durable neuromodulation in nonhuman primates. This noninvasive system can also be applied to subjects with neurological and psychiatric disorders, to modulate specific deep brain targets with the precision and flexibility not previously possible.

Introduction

Nearly one in four people lives with a significant neurological or psychiatric disorder[1,2]. The economic cost to society will reach $ 6.0 trillion by 2030; more than cancer, cardiovascular diseases, and diabetes combined[3]. Approximately one in three patients across neurological and psychiatric conditions does not respond to drugs or has intolerable side effects[4–13].

Precision medicine provides these patients with new treatment options. With respect to disorders of brain function, precision medicine aims to selectively treat the neural source, thus improving the efficacy and curbing the side effects associated with current systemic therapies. A recently developed approach based on noninvasive and focal form of energy has laid a path toward such treatments. In particular, transcranial focused ultrasound offers noninvasive, focal, and flexible treatments of specific brain sites[14–16]. Depending on stimulus duration, ultrasound modulates neural activity[17–23] or induces changes in functional connectivity[24–26] (Figure 1, top). In addition, when combined with nanoparticles or microbubbles, ultrasound can be used to deliver drugs, genes, or stem cells selectively into the specified target/s. This can be achieved by releasing drugs from nanoparticle carriers,[15,27–30] or using microbubbles to temporarily disrupt the blood brain barrier[31,32] and so deliver large agents that would not pass otherwise (Figure 1, bottom). Thus, this form of energy provides novel therapeutic options for the millions of patients who are currently not adequately treated.

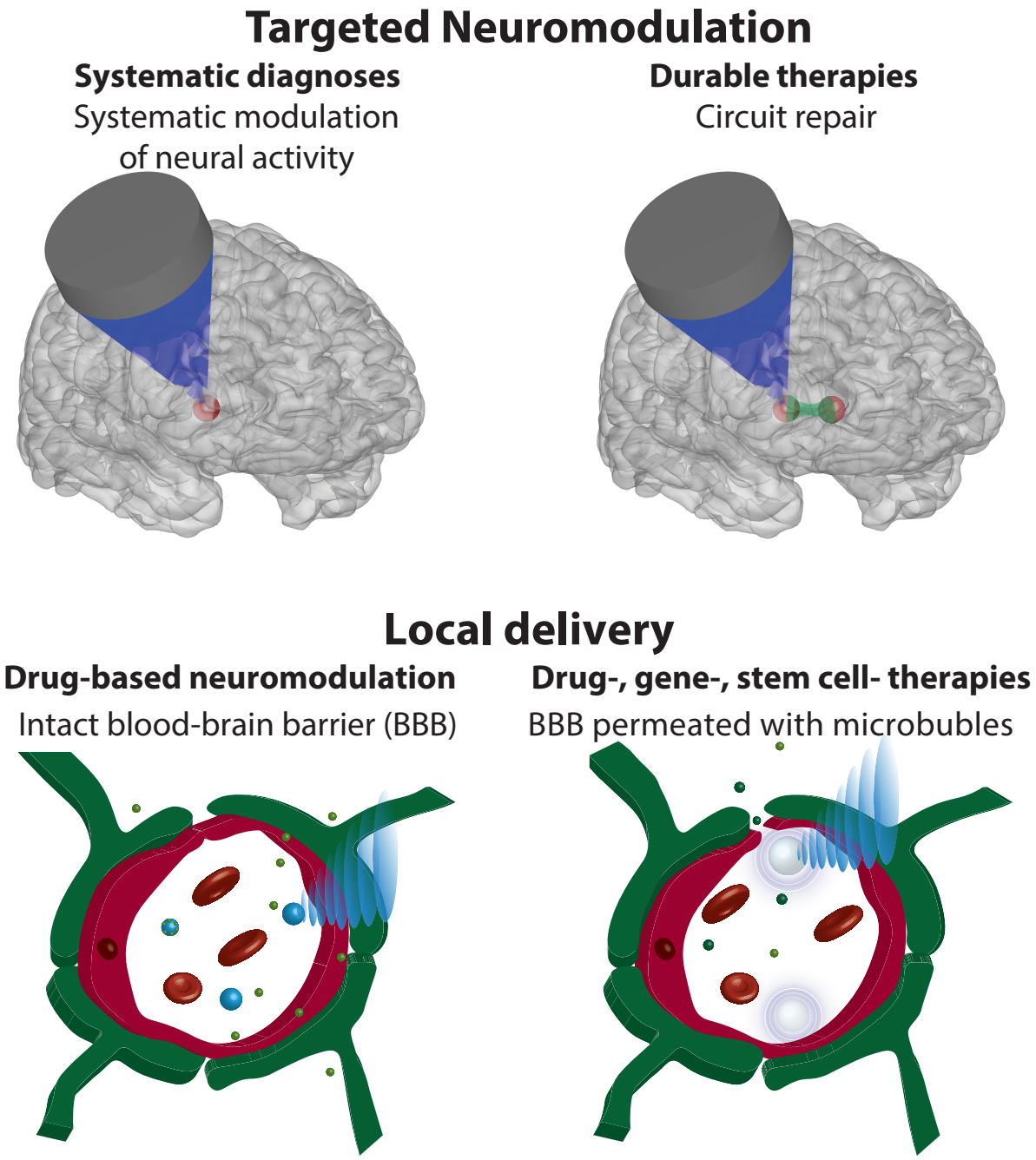

Figure 1. Treatment options enabled by low-intensity transcranial ultrasound.
Brief, millisecond-second ultrasound stimuli modulate neural activity in a transient fashion. This effect, when coupled with successive targeting of individual circuit candidates, provides a tool to dissect circuit function and dysfunction (top left). Ultrasound delivered into a target for minutes induces neuroplastic changes in the target. This could be used for durable reset of the malfunctioning circuits (top right). To further increase the specificity of these effects, ultrasound can be combined with drug-carrying nanoparticles that release their cargo specifically at the ultrasound target (bottom left). If agents that do not naturally cross the blood-brain barrier (BBB) are to be delivered into a target, ultrasound can be combined with microbbubles that—upon sonication—transiently permeate the BBB (bottom right).

However, these applications are limited by technological challenges. A key requirement for the success of the ultrasound-based therapies is the ability to target a specified site flexibly and reproducibly. This flexibility is critical given that the neural sources of many psychiatric and neurological disorders are poorly understood and vary from individual to individual[33–39]. The systems that could provide this functionality—phased arrays—are currently only designed for ablative treatments. However, ablative systems are expensive, require continuous MR-imaging, and have a limited treatment envelope in the center of the brain[14].

We developed a system that provides both noninvasive and flexible targeting of deep brain circuits. The platform enables an operator to specify one or more targets, together with the desired timing and ultrasonic waveform, in software. The design is MR-compatible, which enables researchers and clinicians to confirm precise targeting. The system features imaging functionality that ensures reproducible positioning of the device and validates the quality of the ultrasound coupling to subject's head. We validated these capabilities in nonhuman primates (NHPs). The system can be used to systematically study the effects of specific ultrasonic protocols in NHPs or other large animals. Ultimately, the system will be used to provide precision treatments to patients who are currently out of options.

Results

We developed a practical and affordable platform that delivers focused ultrasound into specified deep brain targets remotely, with the skull and skin intact (Figure 2, top). The targets of the ultrasound are specified in software. The software can flexibly target individual sites in sequence (Figure 2, bottom) or simultaneously.

We validated the function of this platform in a scenario that approximates the ultimate applications in awake patients. Specifically, we used the platform to programmatically deliver focused ultrasound of specific parameters into the left and right LGN while we assessed the effects of the ensuing neuromodulation on behavior. Previous studies have shown that continuous stimuli tend to excite neurons whereas pulsed stimuli, at low duty cycle values, tend to inhibit neurons[40]. In this study, we therefore tested the effects of two values of duty cycle, 10% and 100%.

We found that brief, 300 ms pulses of ultrasound directed into the left and right LGN transiently modulated choice behavior in a NHP. The animal was asked to look at a left or a right target, whichever appeared first. We quantified effects of neuromodulation in the controlled condition in which both targets appeared at the same time. We quantified the proportion of choices of each target when the left LGN was stimulated, when the right LGN was stimulated, and plot the proportion of choices of the contralateral target for these conditions pooled (Figure 3).

In line with the previous suggestion[40], we found that the stimulus pulsed at 10% duty cycle induces a significant ($p = 0.011$, two-sided t-test, $n = 106$) ipsilateral bias, consistent with an inhibition or disruption of the neural activity in the target circuit. The continuous stimulus, for the relatively low pressure used in this initial evaluation, failed to produce a significant effect ($p = 0.52$, two-sided t-test, $n = 285$).

Notably, in this analysis, we only compare effects for trials in which there always was an ultrasound stimulus (either a left or the right LGN was sonicated). This controls for potential generic artifacts that can be associated with ultrasound[41,42]. In addition, we found a significant difference between the two stimulus kinds (blue vs. red in Figure 3; $p = 0.012$; two-sided t-test). This provides additional control—there is a double dissociation of the behavioral bias through the stimulus kind. Interestingly, the stimulus that delivered 10 times less energy into the target (10% duty) produced much stronger effect compared to the more potent 100% duty stimulus. This corroborates the notion that duty cycle constitutes a critical variable in the neuromodulatory effects of ultrasound, and the growing consensus that the effects of low-intensity

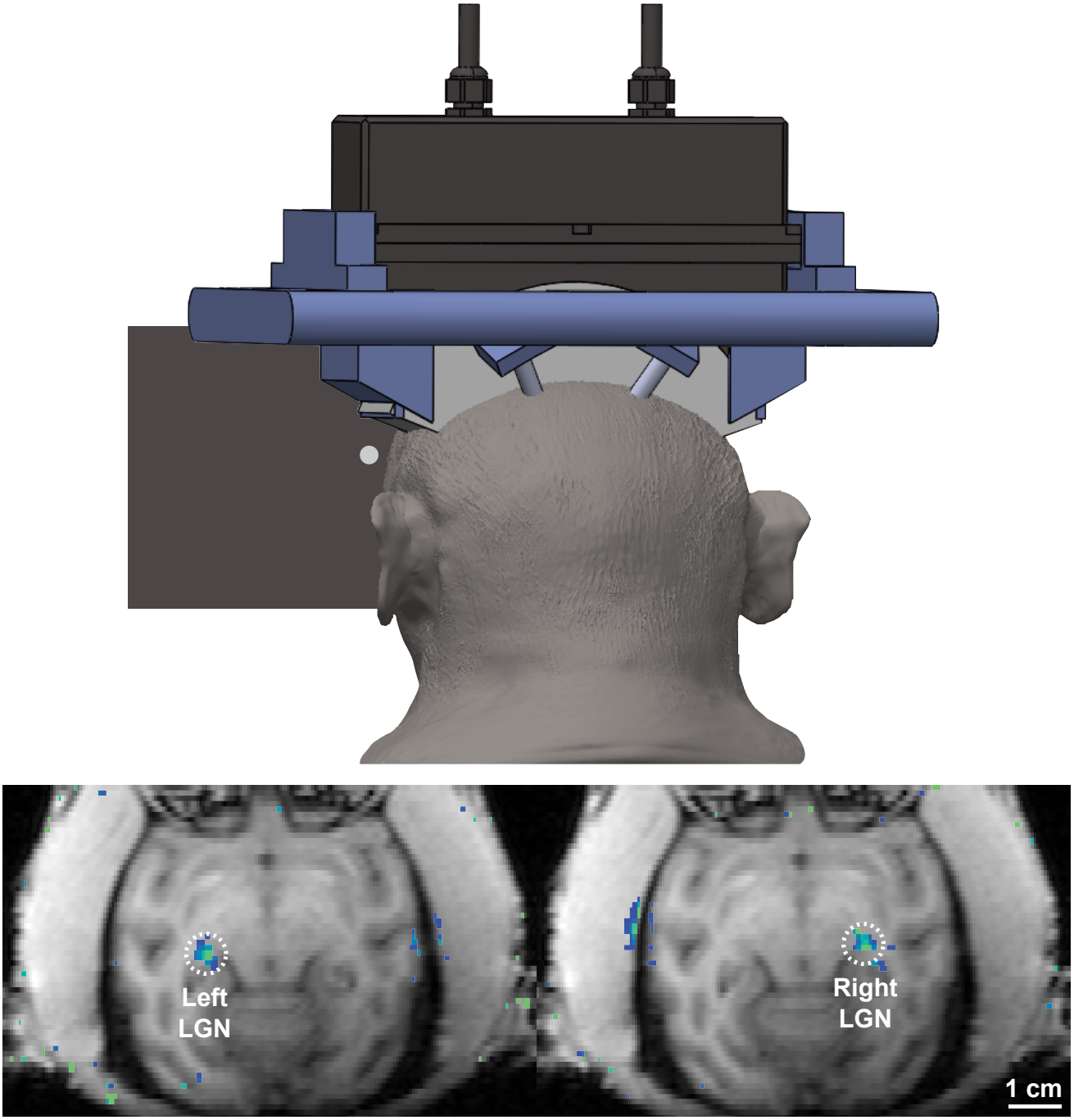

Figure 2. Platform for Incisionless, Targeted and Flexible Brain Interventions.
Top: The platform is attached to the head of a NHP to provide reproducible targeting of deep brain circuits while the subject engages in behavioral tasks.
Bottom: The targets of the ultrasound are specified programmatically. This figure shows selective targeting of the left and right lateral geniculate nucleus (LGN). The platform can be used to target multiple sites in rapid sequence or simultaneously. The images were acquired using MRI thermometry (see Methods).

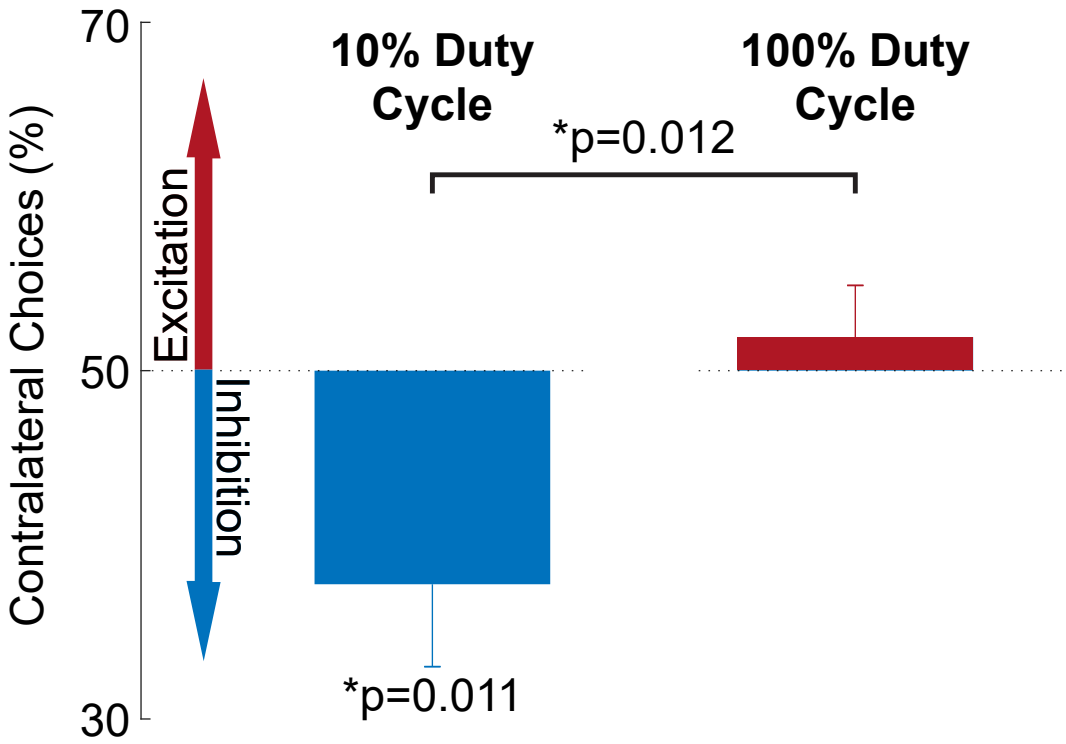

Figure 3. Application of the platform to modulate deep brain nuclei in awake NHPs. Brief, low-intensity ultrasound (300 ms, 650 kHz, 750 kPa pressure at target) was delivered into the left or right LGN every 6-14 s. The side of the stimulation was randomized. The animal was deciding whether to look at a left or a right target. When both targets appeared at the same time, the animal chose both targets at approximately equal proportion. The brief, low-intensity ultrasonic pulses were able to change that choice proportion. Specifically, the stimulus of 10% duty induced an ipsilateral bias, suggesting an inhibition or perturbation of neural activity within the LGN. This effect was significant (see figure; two-sided t-test). Reversely, a continuous stimulus (100%) duty produced a non-significant trend toward an excitation. The difference between the two effects was also significant (two-sided t-test).

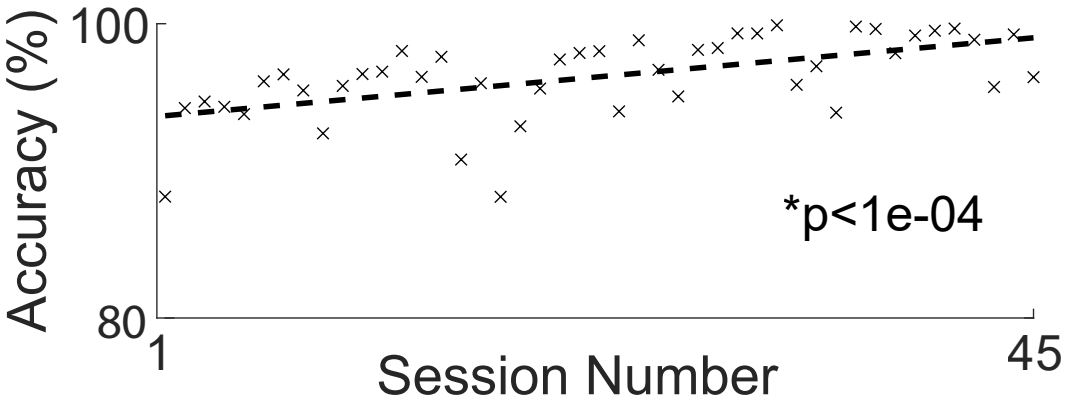

Figure 4. Safety of repeated daily insonations. Damage to the LGN would cause a dramatic decline in the subject's visual discrimination performance. We see the opposite, with the subject improving day by day. This demonstrates that the repeated neuromodulation was safe at the behavioral level. *p*: significance of linear fit.

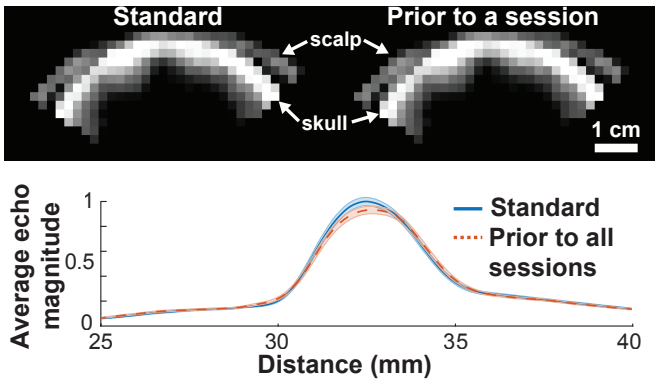

Figure 5. Validation of positioning and coupling. Prior to each session, the platform is operated in imaging mode. **Top:** The imaging reliably detects the location of the scalp and the skull. **Bottom:** The timing of the echoes received from the skull provide information on the position of the device with respect to the skull; their magnitude evaluates the quality of ultrasound coupling to the subject's head.

ultrasound are of mechanical, as opposed to thermal, nature[16,43–45].

The subject's continual improvement in task performance (Figure 4) during trials without ultrasound stimulus demonstrates the safety of repeated sonication over many days. Damage to the LGN would result in a decrease in the subject's accuracy but our data show the opposite effect, with the subject demonstrating significant improvement ($p<1e-4$, measured using a linear hypothesis test) over the course of the study. This result confirms and extends previous findings of the safety of acute sonication[46,47], demonstrating the safety of chronic ultrasound neuromodulation stimulus.

Repeated delivery of ultrasound into the brain rests on reproducible positioning of the stimulation device and on good coupling of the transducer face to the subject's skin. To address these critical aspects of ultrasound delivery, we equipped the platform with imaging functionality that ensures reproducible positioning with respect to the skull and quality coupling (Figure 5). In particular, the device also has a receive capability that together with the transmit function can be used for pulse-echo imaging. The ultrasound images acquired during each session are compared with a standard taken during an MRI imaging session that validated the targeting. This way, the operator can confirm an accurate placement of the array from session to session. In addition, the magnitude of the received echoes (Figure 5, bottom) provides information on the quality of the coupling.

Discussion

We developed and validated a practical, affordable, and MRI-compatible platform that delivers ultrasound through the intact skull and skin on command into single or multiple brain targets in awake subjects. The platform unleashes the full potential of ultrasound: targeted noninvasive interventions deep in the brain. No other approach can offer this desirable intersection of strengths (Figure 6).

Our platform can power the novel treatments afforded by focused ultrasound (Figure 1). The programmatic targeting provides the sorely needed tool to determine which neural circuits should be treated in a given patient. Such functionality requires that brief ultrasonic pulses modulate the desired targets reliably and reversibly. We have indeed demonstrated, in an awake NHP, that ultrasound can be used to robustly and reversibly modulate deep brain targets and the associated behavior (Figure 3). We will use the platform, which can deliver a large number of ultrasonic stimuli into the same target/s day by day, to determine which parameters inhibit and excite neurons most effectively (Figure 3). We will now systematically vary not only the duty cycle, but also the frequency and the intensity of the ultrasound.

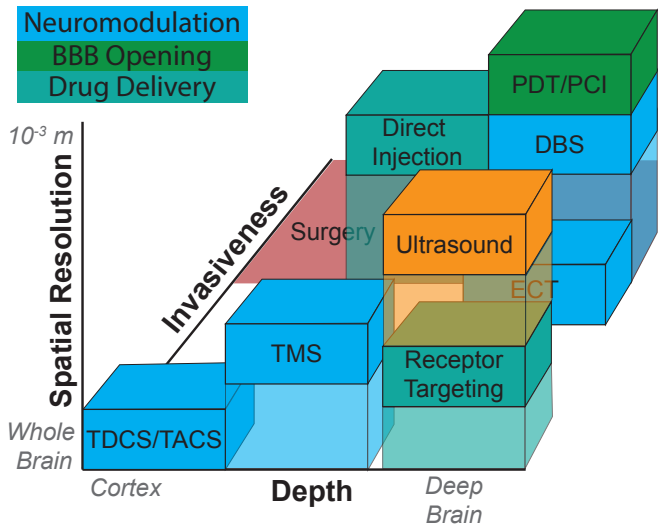

Figure 6. Ultrasound Uniquely Combines Noninvasiveness, Focus, and Depth Penetration.
Abbreviations: DBS: deep brain stimulus; ECT: electro-convulsive therapy; PDT: photodynamic therapy; PCI: photochemical internalization; TMS: transcranial magnetic stimulation; TDCS/TACS: transcranial direct/alternating current stimulation.

The data in Figure 3, collected over 17 days, demonstrates that the platform can be used to reproducibly deliver ultrasound into the target/s each day.

Besides the tremendous opportunity to dissect circuit function and dysfunction, the platform enables researchers to systematically investigate the neuroplastic effets that have been associated with appreciable ultrasound exposures[25,48–53]. Specifically, we will measure effects on behavior before, during, and after sustained stimulation protocols. This way, we will answer, in the primate brain, two key questions regarding this approach—the effect duration and long-term safety of sustained exposure.

The platform provides sufficient pressure output to release drugs into a specified neural circuit during awake behavior. The awake setup enables investigators to quantify the efficacy and duration of the neuromodulatory effects induced by specific neuromodulatory drugs, such as propofol[27,54] or ketamine. In addition, the behavioral readout can be used to assess the safety of the release at the functional level. For instance, damage of the LGN would result in profound degradation of the animal's discrimination ability[55,56].

These protocols can similarly be used to assess the efficacy and safety of cargo delivery across the blood-brain barrier (BBB). To achieve robust therapeutic effects, agents, such as chemotherapy, will likely need to be delivered across the BBB repeatedly and over many sessions. This may raise safety concerns[57]. Our reproducible targeting platform opens doors to systematic investigation of the effects of repeated BBB opening.

Together, the platform described here provides the capacity to implement several, if not all, of the novel ultrasound-based approaches to targeted yet noninvasive brain intervention (Figure 1). The platform, along with the research outlined in this section, has the potential to bring these precision treatments to the millions of people with treatment-resistant neurological and psychiatric conditions.

Methods

Animals

One subject participated in this study (male *macaca mulatta*, age 6 years, weight 8 kg). The procedures were approved by the Institutional Animal Care and Use Committee of the University of Utah.

Platform positioning and Head Fixation

We developed an apparatus that ensures reproducible positioning of the platform with respect to the head from session to session, and at the same time allows us to head-fix NHPs and engage them in behavioral tasks. To achieve that, we developed a custom head frame that is attached to the skull via four titanium pins (Gray Matter Research, Bozeman, MT). Each pin is attached to the skull using three screws. The frame is attached to a primate chair using two steel bars, mounted into the left and right side of the frame. Coupling of the transducer to the skull is achieved using a 6% polyvinyl alcohol (PVA) gel[58]. The subject's hair is shaved prior to each session. Shaving may not be necessary in the ultimate human applications; the platform detect the quality of the coupling and aberration due to the hair, and adjust the emitted ultrasound amplitude accordingly.

In each session, the system verifies the device placement with respect to the head and the quality of the acoustic coupling using ultrasound imaging. Specifically, the system measures the distance between the transducer and the skull at six distinct locations. A pulse-echo measurement, performed on a 3x3 grid of elements, provides an estimate of the location of the skull relative to the transducer. Using this measurement, we perform data collection only when maximum error is less than one wavelength (2.3 mm at 650 kHz), and when the average error is smaller than half the wavelength (1.15 mm). The coupling is verified visually (Figure 5, top) and by measuring the intensity of the echo integrated across the array (Figure 5, bottom). Coupling is considered poor if the intensity of the echo falls bellow 30% of the standard. This system provided highly reliable placement of the transducer and the coupling gel. Only two out of 36 sessions were rejected due to poor placement of the transducer or inadequate coupling.

MR Imaging

The system is fully MRI-compatible. Accurate targeting of specific deep brain regions can therefore be validated using MRI, such as MR thermometry or MRI ARFI. We used MR thermometry. In this approach, a continuous, 5-second sonication is sufficient to increase temperature at the focal spot by about 2°C, enabling visualization of the focus without inducing long-term changes in the neural tissue.

All scans were performed using a 3T MRI scanner (Trio, Siemens Medical Solutions, Erlangen, Germany) with a 4-channel flex coil wrapped underneath the animal's head. High resolution 3D T1-weighted images were used for anatomical imaging and target identification; Magnetization Prepared Rapid Acquisition Gradient Echo (MPRAGE), TR=1900 ms, TE=3.39 ms, TI-900 ms, BW=180 Hz/pixel, flip angle 9°, FOV = 192x192x120 mm, resolution 1x1x1 mm, acquisition time 5:12 min. MR thermometry was performed with a 3D gradient recalled segmented echo planar imaging pulse sequence; TR=24 ms, TE=11 ms, BW=592 Hz/pixel, flip angle 12°, echo train length = 5 with monopolar readout, FOV = 144x117x36 mm, resolution 1.5x1.5x3.0 mm, acquisition time 4.6 s per dynamic image.

Acoustic Intensity at Target

The MRI thermometry additionally allowed us to compute the ultrasound pressure delivered in the target. Assuming negligible conduction and perfusion and a continuous sonication, the acoustic intensity, I, is related to the temperature rise, ΔT, by[59]

$$I = \frac{\rho C \Delta T}{\Delta t \alpha}, \tag{1}$$

where ρ, C, and α are the density, specific heat capacity, and acoustic absorption of the tissue and Δt is the time in which the temperature increase occurs. To minimize the effects of conduction and perfusion ΔT is assumed to be the maximum temperature measured in the seventh dynamic (the first dynamic in which the ultrasound is on). The center of k-space is acquired 2.3 seconds into each acquisition. Thus, Δt was set to 2.3 s. We assumed a density of 1046 kg/m^3, a specific heat capacity of 3630 J/K, and an acoustic absorption of 3.9 Np/m.

Stimulation Parameters

The transducer (Doppler Electronic Technologies, Guangzhou, China) can produce focal pressures greater than 3 MPa at its 650 kHz center frequency. All stimuli used 650 kHz. The pulsed stimulus (10% duty) used a 500 Hz pulse repetition frequency. The peak focal pressure was 770 and 650 kPa in the right and left LGN respectively. The half power beam width for the right LGN was 1, 3.75, and 3.75 mm in the left/right, anterior/posterior, and superior/inferior dimensions, respectively. The free field pressure, measured using a hydrophone, is 2.4 MPa at the location of the left and right LGN. Thus, the MR thermometry measurements suggest that about 30% of the pressure reaches the target through the individual layers. It is worth noting, nonetheless, that this estimate likely underestimates the actual pressure at target. In particular, the temperature measured by the MR is averaged within a voxel; the actual peak temperature within the voxel is higher than the average. In addition, a portion of the energy is distributed to the thermal conduction and vascular convection.

Task

We trained one NHP to perform a visual choice task. This task was used in many previous studies (e.g.,[18,60]). Briefly, the subject was seated in a comfortable primate chair and was presented with visual stimuli shown on a monitor. In the task, the subject first fixates a central target. Following its offset, one target appears on the left and one target on the right side of the screen. There is a brief, controllable delay between the onset of the two targets, which can range from -40 to 40 ms. We varied the location of the targets within 2.5 visual degrees to circumvent adaptation. The sonication of the left and right LGN was randomly interspersed with trials in which no ultrasound was delivered. In an ultrasound trial, a 300 ms stimulus was delivered 150 ms before the fixation point offset. The subject receives a liquid reward if he looks at the target that appeared first within 2 s. In the key condition in which both targets appear at the same time and during which we quantify the effect of ultrasound, the subject is rewarded for either choice.

Acknowledgments

This development of the platform and its application in NHPs was supported by the National Institute of Neurological Disorders and Stroke, Grants 5R00NS100986 and F32MH123019. We thank Tyler Davis and Eric Burdett for facilitating this work.

References

1. Lancet. Life, death, and disability in 2016. *The Lancet* **390**, 1084–1423 (2017).
2. Ahrnsbrak, R., Bose, J., Hedden, S., Lipari, R. & Park-Lee, E. Key substance use and mental health indicators in the United States: Results from the 2016 National Survey on Drug Use and Health. *Cent. for Behav. Heal. Stat. Qual. Subst. Abus. Mental Heal. Serv. Adm. Rockville, MD, USA* (2017).
3. Bloom, D. *et al.* Geneva: World Economic Forum, 2011. The global economic burden of non-communicable diseases (2016).

4. Bystritsky, A. Treatment-resistant anxiety disorders. *Mol. psychiatry* **11**, 805–814 (2006).
5. Al-Harbi, K. S. Treatment-resistant depression: therapeutic trends, challenges, and future directions. *Patient preference adherence* **6**, 369 (2012).
6. Jaffe, D. H., Rive, B. & Denee, T. R. The humanistic and economic burden of treatment-resistant depression in europe: a cross-sectional study. *BMC psychiatry* **19**, 247 (2019).
7. Lyons, K. E. & Pahwa, R. Deep brain stimulation and essential tremor. *J. clinical neurophysiology* **21**, 2–5 (2004).
8. Zesiewicz, T. A., Chari, A., Jahan, I., Miller, A. M. & Sullivan, K. L. Overview of essential tremor. *Neuropsychiatr. disease treatment* **6**, 401 (2010).
9. Elias, W. J. *et al.* A pilot study of focused ultrasound thalamotomy for essential tremor. *New Engl. J. Medicine* **369**, 640–648 (2013).
10. Elias, W. J. *et al.* A randomized trial of focused ultrasound thalamotomy for essential tremor. *New Engl. J. Medicine* **375**, 730–739 (2016).
11. Ferguson, J. M. Ssri antidepressant medications: adverse effects and tolerability. *Prim. care companion to J. clinical psychiatry* **3**, 22 (2001).
12. Karceski, S. C. Seizure medications and their side effects. *Neurology* **69**, E27–E29 (2007).
13. Louis, E. D., Rios, E. & Henchcliffe, C. How are we doing with the treatment of essential tremor (et)? persistence of patients with et on medication: data from 528 patients in three settings. *Eur. journal neurology* **17**, 882–884 (2010).
14. Ghanouni, P. *et al.* Transcranial MRI-guided focused ultrasound: A review of the technologic and neurologic applications. *Am. J. Roentgenol.* **205**, 150–159, DOI: 10.2214/AJR.14.13632 (2015).
15. Wang, J. B., Aryal, M., Zhong, Q., Vyas, D. B. & Airan, R. D. Noninvasive Ultrasonic Drug Uncaging Maps Whole-Brain Functional Networks. *Neuron* **100**, 728–738.e7, DOI: 10.1016/j.neuron.2018.10.042 (2018).
16. Fomenko, A. *et al.* Systematic examination of low-intensity ultrasound parameters on human motor cortex excitability and behavior. *Elife* **9**, e54497 (2020).
17. Fry, W. J. Use of intense ultrasound in neurological research. *Am. journal physical medicine* **37**, 143–7 (1958).
18. Kubanek, J. *et al.* Remote, brain region–specific control of choice behavior with ultrasonic waves. *Sci. Adv.* **6**, eaaz4193, DOI: 10.1126/sciadv.aaz4193 (2020).
19. Deffieux, T., Younan, Y., Wattiez, N., Tanter, M. & Pouget, P. Low-Intensity Focused Ultrasound Modulates Monkey Visuomotor Behavior. *Curr. Biol.* **23**, 2430–2433, DOI: 10.1016/j.cub.2013.10.029 (2013).
20. Tufail, Y. *et al.* Transcranial Pulsed Ultrasound Stimulates Intact Brain Circuits. *Neuron* **66**, 681–694, DOI: 10.1016/j.neuron.2010.05.008 (2010).
21. Lee, W. *et al.* Image-Guided Transcranial Focused Ultrasound Stimulates Human Primary Somatosensory Cortex. *Sci. Reports* **5**, 8743, DOI: 10.1038/srep08743 (2015).
22. Legon, W. *et al.* Transcranial focused ultrasound modulates the activity of primary somatosensory cortex in humans. *Nat. neuroscience* **17**, 322–329, DOI: 10.1038/nn.3620 (2014).

23. Mueller, J., Legon, W., Opitz, A., Sato, T. F. & Tyler, W. J. Transcranial focused ultrasound modulates intrinsic and evoked EEG dynamics. *Brain Stimul.* **7**, 900–908, DOI: 10.1016/j.brs.2014.08.008 (2014).

24. Verhagen, L. *et al.* Offline impact of transcranial focused ultrasound on cortical activation in primates. *eLife* **8**, 1–28, DOI: 10.7554/elife.40541 (2019).

25. Folloni, D. *et al.* Manipulation of subcortical and deep cortical activity in the primate brain using transcranial focused ultrasound stimulation. *Neuron* **101**, 1109–1116 (2019).

26. Bongioanni, A. *et al.* Activation and disruption of a neural mechanism for novel choice in monkeys. *Nature* 1–5 (2021).

27. Airan, R. D. *et al.* Noninvasive Targeted Transcranial Neuromodulation via Focused Ultrasound Gated Drug Release from Nanoemulsions. *Nano Lett.* **17**, 652–659, DOI: 10.1021/acs.nanolett.6b03517 (2017).

28. Rapoport, N., Pitt, W. G., Sun, H. & Nelson, J. L. Drug delivery in polymeric micelles: From in vitro to in vivo. *J. Control. Release* **91**, 85–95, DOI: 10.1016/S0168-3659(03)00218-9 (2003).

29. Rapoport, N. *et al.* Ultrasound-mediated tumor imaging and nanotherapy using drug loaded, block copolymer stabilized perfluorocarbon nanoemulsions. *J. Control. Release* **153**, 4–15, DOI: 10.1016/j.jconrel.2011.01.022 (2011).

30. Lea-Banks, H., O'Reilly, M. A., Hamani, C. & Hynynen, K. Localized anesthesia of a specific brain region using ultrasound-responsive barbiturate nanodroplets. *Theranostics* **10**, 2849–2858, DOI: 10.7150/thno.41566 (2020).

31. Abrahao, A. *et al.* First-in-human trial of blood–brain barrier opening in amyotrophic lateral sclerosis using MR-guided focused ultrasound. *Nat. Commun.* **10**, 1–9, DOI: 10.1038/s41467-019-12426-9 (2019).

32. Hynynen, K., McDannold, N., Vykhodtseva, N. & Jolesz, F. A. Noninvasive MR imaging-guided focal opening of the blood-brain barrier in rabbits. *Radiology* **220**, 640–646, DOI: 10.1148/radiol.2202001804 (2001).

33. Braun, U. *et al.* From maps to multi-dimensional network mechanisms of mental disorders. *Neuron* **97**, 14–31 (2018).

34. Duchowny, M., Jayakar, P. & Levin, B. Aberrant neural circuits in malformations of cortical development and focal epilepsy. *Neurology* **55**, 423–428 (2000).

35. Price, J. L. & Drevets, W. C. Neural circuits underlying the pathophysiology of mood disorders. *Trends cognitive sciences* **16**, 61–71 (2012).

36. Peirs, C. & Seal, R. P. Neural circuits for pain: recent advances and current views. *Science* **354**, 578–584 (2016).

37. Lynall, M.-E. *et al.* Functional connectivity and brain networks in schizophrenia. *J. Neurosci.* **30**, 9477–9487 (2010).

38. Ramasubbu, R. *et al.* Reduced intrinsic connectivity of amygdala in adults with major depressive disorder. *Front. psychiatry* **5**, 17 (2014).

39. Insel, T. R. & Cuthbert, B. N. Brain disorders? Precisely. *Science* **348**, 499–500 (2015).

40. Plaksin, M., Kimmel, E. & Shoham, S. Cell-Type-Selective Effects of Intramembrane Cavitation as a Unifying Theoretical Framework for Ultrasonic Neuromodulation. *eNeuro* **3**, DOI: 10.1523/ENEURO.0136-15.2016 (2016). 978-1-4244-4855-5.

41. Guo, H. *et al.* Ultrasound produces extensive brain activation via a cochlear pathway. *Neuron* (2018).

42. Sato, T., Shapiro, M. G. & Tsao, D. Y. Ultrasonic Neuromodulation Causes Widespread Cortical Activation via an Indirect Auditory Mechanism. *Neuron* **98**, 1031–1041.e5, DOI: 10.1016/j.neuron.2018.05.009 (2018).

43. Tyler, W. J., Lani, S. W. & Hwang, G. M. Ultrasonic modulation of neural circuit activity. *Curr. opinion neurobiology* **50**, 222–231 (2018).

44. Kubanek, J. Neuromodulation with transcranial focused ultrasound. *Neurosurg. Focus.* **44**, E14 (2018).

45. Naor, O., Krupa, S. & Shoham, S. Ultrasonic neuromodulation. *J. Neural Eng.* **13**, 031003 (2016).

46. Tufail, Y. *et al.* Transcranial pulsed ultrasound stimulates intact brain circuits. *Neuron* **66**, 681–694 (2010).

47. Yoo, S.-S. *et al.* Focused ultrasound modulates region-specific brain activity. *Neuroimage* **56**, 1267–1275 (2011).

48. Velling, V. & Shklyaruk, S. Modulation of the functional state of the brain with the aid of focused ultrasonic action. *Neurosci. behavioral physiology* **18**, 369–375 (1988).

49. Dallapiazza, R. F. *et al.* Noninvasive neuromodulation and thalamic mapping with low-intensity focused ultrasound. *J. Neurosurg.* 1–10 (2017).

50. Oh, S.-J. *et al.* Ultrasonic neuromodulation via astrocytic trpa1. *Curr. Biol.* **29**, 3386–3401 (2019).

51. Verhagen, L. *et al.* Offline impact of transcranial focused ultrasound on cortical activation in primates. *Elife* **8**, e40541 (2019).

52. Fouragnan, E. F. *et al.* The macaque anterior cingulate cortex translates counterfactual choice value into actual behavioral change. *Nat. neuroscience* **22**, 797–808 (2019).

53. Khalighinejad, N. *et al.* A basal forebrain-cingulate circuit in macaques decides it is time to act. *Neuron* **105**, 370–384 (2020).

54. Wang, J. B., Aryal, M., Zhong, Q., Vyas, D. B. & Airan, R. D. Noninvasive ultrasonic drug uncaging maps whole-brain functional networks. *Neuron* **100**, 728–738 (2018).

55. Ro, T., Rorden, C., Driver, J. & Rafal, R. Ipsilesional biases in saccades but not perception after lesions of the human inferior parietal lobule. *J. Cogn. Neurosci.* **13**, 920–929 (2001).

56. Schiller, P. H. & Tehovnik, E. J. Cortical inhibitory circuits in eye-movement generation. *Eur. J. Neurosci.* **18**, 3127–3133 (2003).

57. Kovacs, Z. I. *et al.* Disrupting the blood–brain barrier by focused ultrasound induces sterile inflammation. *Proc. Natl. Acad. Sci.* **114**, E75–E84, DOI: 10.1073/pnas.1614777114 (2017).

58. Lee, W., Lee, S. D., Park, M. Y., Yang, J. & Yoo, S.-S. Evaluation of polyvinyl alcohol cryogel as an acoustic coupling medium for low-intensity transcranial focused ultrasound. *Int. J. Imaging Syst. Technol.* **24**, 332–338, DOI: 10.1002/ima.22110 (2014).

59. Pennes, H. H. Analysis of Tissue and Arterial Blood Temperatures in the Resting Human Forearm. *J. Appl. Physiol.* **1**, 93–122, DOI: 10.1152/jappl.1948.1.2.93 (1948).

60. Kubanek, J., Li, J. M. & Snyder, L. H. Motor role of parietal cortex in a monkey model of hemispatial neglect. *Proc. Natl. Acad. Sci. United States Am.* **112**, E2067–E2072, DOI: 10.1073/pnas.1418324112 (2015).